Brain Tumor Pathology (2019) 36:92–101
https://doi.org/10.1007/s10014-019-00338-x

ORIGINAL ARTICLE

Review of ependymomas: assessment of consensus in pathological diagnosis and correlations with genetic profiles and outcome

Atsushi Sasaki[1] · Junko Hirato[2] · Takanori Hirose[3] · Kohei Fukuoka[4,9] · Yonehiro Kanemura[5,9] · Naohito Hashimoto[1] · Yoshinori Kodama[6] · Koichi Ichimura[4,9] · Hiroaki Sakamoto[7,9] · Ryo Nishikawa[8,9]

Received: 14 February 2019 / Accepted: 17 March 2019 / Published online: 30 March 2019

Abstract

We focused on histological and immunohistochemical characteristics of ependymoma (EPN) with molecular profiles to develop more reproducible criteria of the diagnosis. Three expert neuropathologists reviewed the pathology of 130 samples from the Japan Pediatric Molecular Neuro-Oncology Group study. Confirmed cases were assessed for histology, surrogate markers, molecular subgrouping, and survival data. We reached a consensus regarding the diagnosis of EPNs in 100% of spinal cord tumors and 93% of posterior fossa (PF) tumors that had been diagnosed as EPNs by local pathologists, whereas we reached a consensus regarding only 77% of the local diagnosis of supratentorial (ST) EPNs. Among the PF-EPNs, most of anaplastic ependymomas (AEPNs) were defined as EPN-A by methylation profiling, which was significantly correlated with the subgroup assignment. Regarding prognosis, the overall survival of patients with PF-EPN was significantly better than that of patients with PF AEPN ($p=0.01$). Histologically, all ependymoma, *RELA* fusion-positive (EPN-RELA) qualified as Grade III. Both L1 cell adhesion molecule and nuclear factor kappaB p65 antibodies showed good sensitivity for detecting EPN-RELA. This study indicated that the expert consensus pathological diagnosis could correlate well with the molecular classifications in EPNs. ST EPNs should be diagnosed more carefully by histological and molecular analyses.

Keywords Ependymoma · Immunohistochemistry · RELA · Posterior fossa · Supratentorial · L1CAM · NF-kB

✉ Atsushi Sasaki
asasaki@saitama-med.ac.jp

1 Department of Pathology, Saitama Medical University, 38 Morohongo, Moroyama-machi, Saitama 350-0495, Japan

2 Department of Pathology, Gunma University Hospital, Maebashi, Gunma, Japan

3 Department of Pathology for Regional Communication, Kobe University, Kobe, Hyogo, Japan

4 Division of Brain Tumor Translational Research, National Cancer Center Research Institute, Tokyo, Japan

5 Department of Neurosurgery and Institute for Clinical Research, Osaka National Hospital, Osaka, Japan

6 Department of Pathology and Applied Neurobiology, Graduate School of Medical Science, Kyoto Prefectural University of Medicine, Kyoto, Japan

7 Department of Pediatric Neurosurgery, Osaka City General Hospital, Osaka, Japan

8 Department of Neuro-Oncology/Neurosurgery, Saitama Medical University International Medical Center, Saitama, Japan

9 Japan Pediatric Molecular Neuro-Oncology Group (JPMNG), Tokyo, Japan

Introduction

Ependymoma (EPN) is a histologically defined glioma subtype that arises in the three anatomic areas of the central nervous system (CNS): − 30% in the supratentorial (ST) compartment, 60% in the posterior fossa (PF), and 10% in the spinal cord (SC) [1]. EPNs are relatively uncommon, but can occur in patients of any age. PF-EPNs are more common in children, and the incidence of EPNs depends on histological variant, molecular group, and location. According to recent molecular analyses, ST and PF-EPNs are distinct diseases but histopathologically similar. Compared with the outcomes for other pediatric brain tumors, the outcome for EPNs is relatively poor, such that the 5-year overall survival (OS) rate for childhood EPNs is approximately 39–73% [2–5]. Postoperative, targeted therapeutic options for high-risk EPNs will be required to achieve further improvement in prognosis.

In the 2016 WHO classification of the CNS (CNS WHO 2016), EPNs were categorized into five subtypes: (1) subependymoma (SE; Grade I), (2) myxopapillary EPN (MPE;

Grade I), (3) EPN, (4) EPN, *RELA* fusion-positive (EPN-RELA) (Grade II or III), and (5) anaplastic EPN (AEPN). Histopathological diagnosis and, thus, distinguishing EPNs from many other brain tumors are the first step in treating patients with EPNs. However, diagnosing EPNs, particularly AEPNs, can be difficult, because there is no clear consensus on the required criteria and because of questionable clinical utility of these criteria [6, 7]. Thus, progress has been made in characterizing the molecular genetic abnormalities associated with pediatric and adult EPNs. A recent paper reported the current consensus on the clinical management of intracranial EPN and its distinct molecular variants, which consisted of ST-EPN-RELA, ST-EPN-YAP1, PF-EPN-A, and PF-EPN-B [8]. However, despite the increasing recognition of the importance of these molecular markers, they currently are not routinely determined in clinical practice [9], and a more reproducible and therapy-related classification and grading scheme have yet to be published.

EPN-RELA has been accepted as one genetically defined EPN subtype in the CNS WHO 2016. This variant accounts for approximately 70% of all childhood ST tumors, and a significant proportion of EPN-RELA (24%=20/84 cases) cases was found in adults [10]. A relatively large study revealed that patients with EPN-RELA present with a poor prognosis with 5-year progression-free survival (PFS) and 10-year PFS rates of 29% and 19%, respectively [11]. However, inconsistent with this result, Figarella-Branger [12] found that the prognostic values of RELA fusions in EPNs were 67.5% and 57.9% at the 5- and 10-year PFS, respectively, which suggested that clear cell EPNs (CCEs) with branching vessels might represent a subset of ST-EPN-RELAs with a more favorable prognosis. According to the WHO classifications, a major proportion of ST-EPN-RELA are assigned to AEPN WHO grade III [11–14]. Concerning a potential surrogate immunohistochemical marker for this variant, the specificity of L1 cell adhesion molecule (L1CAM) expression [10] has yet to be fully elucidated. A recent study emphasized the usefulness of IHC with anti-nuclear factor kappaB (NF-kB) p65 antibody to pinpoint cases with a *C11orf95-RELA* fusion [12]. One of the remaining ST subgroups is ST-EPN-YAP1 which shows an extremely favorable clinical outcome. However, no dominant histologic grade has been determined regarding the morphological characteristics of ST-EPN-YAP1. For PF-EPNs, LAMA2 and NELL2 expression was previously suggested as immunohistochemical markers for PF Group A and Group B EPNs, respectively [15].

The Japan Pediatric Molecular Neuro-Oncology Group (JPMNG) was established to facilitate molecular genetic analysis of pediatric brain tumors, and in doing so, the JPMNG collected 130 samples of locally diagnosed EPNs. First, in this study, three expert neuropathologists diagnosed tumors according to proposed EPN criteria and without any molecular/genetic information. Then, using a representative specimen of the consensus diagnosis, we investigated the efficacy of the surrogate markers, L1CAM and NF-kB p65, and compared the prognosis of each EPN group as diagnosed by central review and molecular/genetic analyses.

Materials and methods

Tumor samples

A total of 130 tumors, including 129 EPNs and one ependymoblastoma (EBL), diagnosed by local pathologists were collected from the JPMNG for this study. There were 123 patients and 130 tumor samples, and the tumors were distributed in the following locations (number of samples): ST (43), PF (72), and SC (15). This study was approved by the ethics committees of the National Cancer Research Center and the respective local institutional review boards. For the central pathology review, research centers were required to submit hematoxylin and eosin (H&E)-stained slides. Glass slides that were immunohistochemically stained with antibodies against GFAP, Olig2, EMA, and Ki-67 were also available in many cases. Three neuropathologists (AS, JH, and TH) were asked to individually diagnose each case without knowledge of the molecular data. In addition, the neuropathologists were asked to score histological features (i.e., cell density, perivascular rosette, true rosette, mitotic counts/10 HPF, microvascular proliferation, and necrosis) and the Ki-67 labeling index. High cellularity included focal hypercellular nodules as well as diffuse hypercellularity (high cell density predominantly throughout the tumor tissue). A joint review was conducted to ascertain the histological features with a multihead scope.

IHC and immunofluorescence of surrogate markers

IHC was performed on the formalin-fixed, paraffin-embedded (FFPE) tissue slides. Primary antibodies used in this study are as follows: monoclonal mouse anti-laminin alpha-2 (LAMA2) antibody (Ab) (2D4, Abnova, Taipei, Taiwan; 1:600 dilution), rabbit polyclonal anti-neural epidermal growth factor like-2 (NELL2) Ab (Abcam Inc., Cambridge, MA, USA; 1:250 dilution), monoclonal mouse anti-L1CAM Ab (UJ127, Novus Biologicals, Littleton, CO, USA; 1:50 dilution), and monoclonal rabbit anti-NF-kB p65 Ab (D14E12, Cell Signaling Technology, Danvers, MA, USA; 1:400 dilution). Abs against LAMA2 and NELL2 were used to stain specimens from 32 patients. An Ab against L1CAM was used for staining specimens from 60 patients, including 12 patients who had undergone surgery at the Saitama Medical University International Medical Center from 1998 to 2013, while an RELA Ab was used to stain specimens from the 12 Saitama patients. The LAMA2 and NELL2 staining protocol was as follows: on a Ventana Benchmark

platform (Ventana Medical System, Tuscon, AZ, USA), samples were pretreated by incubating in EDTA buffer pH 8.5 for 64 min at 95 °C or in citrate buffer pH 6.0 for 56 min at 95 °C. Next, samples were incubated with primary Abs for 60 min at room temperature (RT) and were developed with an Ultraview-HRP kit, which included incubation with the appropriate secondary Ab for 30 min at RT, and then, a hematoxylin (Hx) counterstain was applied. L1CAM was stained by either automated or manual modalities using a Ventana Benchmark platform. For the latter method, after deparaffinization, antigen retrieval was performed by autoclaving (121 °C, 10 min, citrate buffer pH 6.0). Immunoreactivity was visualized by automated or manual staining with a Histofine Simple Stain MAX-PO (Nichirei, Tokyo, Japan). NF-kB p65 was stained by the manual method.

Nuclear staining of NF-kB p65 was rated positive, whereas membranous staining of L1CAM was rated as positive.

For immunofluorescence, sections of two cases of EPN-RELAs were double-labeled with L1CAM and NF-kB p65 antibodies, as previously described [16].

Molecular analyses

Molecular analyses were performed in 113 locally diagnosed ependymal tumors, as described previously [17]. In brief, genome-wide methylation analysis was performed using an Illumina Human Methylation 450K BeadChip array (Illumina, San Diego, CA, USA) as previously described [11, 17]. Probes (total 3,932) showing a high standard deviation (SD > 0.25) on CpG islands were selected for analyzing PF-EPN classification. A combination of RT-PCR, break-apart fluorescence in situ hybridization (FISH), and RNA sequencing was performed to detect *C11orf95-RELA* fusion genes [10].

Statistical analysis

Subgroup comparison was performed using Fisher's exact test. OS was defined as the probability of survival, with only death as an event. PFS was defined as the probability of being alive and free of progression or relapse. Survival curves were plotted using the Kaplan–Meier method. The log-rank test and Cox proportional hazards model were used to detect differences in survival between different groups of patients.

Results

Concordance of central diagnosis and local diagnosis with anatomical location

We reached a consensus regarding the diagnosis of EPNs in 100%, 93%, and 77% of the SC, PF, and ST tumors, respectively, that had been diagnosed by local pathologists (Fig. 1), and no subependymoma was found. Of the 43 ST-EPN cases identified by central pathology review, only 33 fulfilled the EPN diagnostic criteria. The central pathology excluded the following diagnoses: glioblastoma, malignant gliomas with a primitive neuronal component, pilocytic astrocytomas, medulloblastomas, atypical teratoid/rhabdoid tumors, and high-grade malignant tumors, not otherwise specified. We established the diagnosis of AEPN in 1 SC tumors, 42 PF tumors, and 28 ST tumors. Based on associations with anatomical location, histology, and molecular alterations, as outlined below, we annotated 94 tumors as SC-EPN ($n = 13$), SC-MPE ($n = 1$), PF-EPN-A ($n = 45$), PF-EPN-B ($n = 15$), ST-EPN-RELA ($n = 19$), and ST-EPN-YAP1 ($n = 1$) according to a molecular subgrouping of EPNs [11].

Histopathology review

Epithelial features, such as "true ependymal rosettes" or "canals", were observed in only a minority of cases. Regarding AEPNs, while diffuse hypercellularity was observed in 72.7% of cases, focal hypercellular nodules were observed in 27.3% of cases. Approximately 60% of AEPN cases underwent greater than 10 mitoses per 10 high-power field (HPF), while 25% had mitoses between 5 and 10 per 10 HPF, and 15% had fewer than 5 per 10 HPF. Among Grade II EPNs, approximately 40% tumors exhibited mitoses fewer than 5 per 10 HPF, but none had mitoses greater than 10 per 10 HPF. All the AEPN cases showed high MIB-1 LI (> 10%). Among AEPN cases, bonafide microvascular proliferation (MVP) was present in 76% of cases, and necrosis was present in 83% of cases. Only 7% of cases had classical palisading necrosis. Thus, the diagnostic criteria for AEPN were proposed when an ependymal tumor showed a markedly increased mitotic activity (10 or more mitoses per 10 HPFs) or the following three features: (1) high cellularity, (2) increased proliferation (5–9 mitoses per 10 HPFs and/or high MIB-1 labeling index > 10%), and (3) MVP or necrosis (Table 1).

Molecular typing and histology/grading

Among PF-EPNs diagnosed by the central review and molecular analyses, 38 of 45 PFA tumors (84%) were defined as Grade III, while most PFB were Grade II (12 of 15; 80%) ($p < 0.0001$). All EPN-RELA was classified as Grade III (19 of 19; 100%), and 19 of 25 ST AEPNs (76%) were characterized by *C11orf95–RELA* gene fusions. The *C11orf95–RELA* gene fusions were present in only ST EPNs, but not in PF/SC EPNs or ST tumors misdiagnosed as EPNs by local pathologists. By histological and molecular analyses, 29 ST EPNs were classified as EPN-RELA (19/29 = 66%), EPN-YAP1

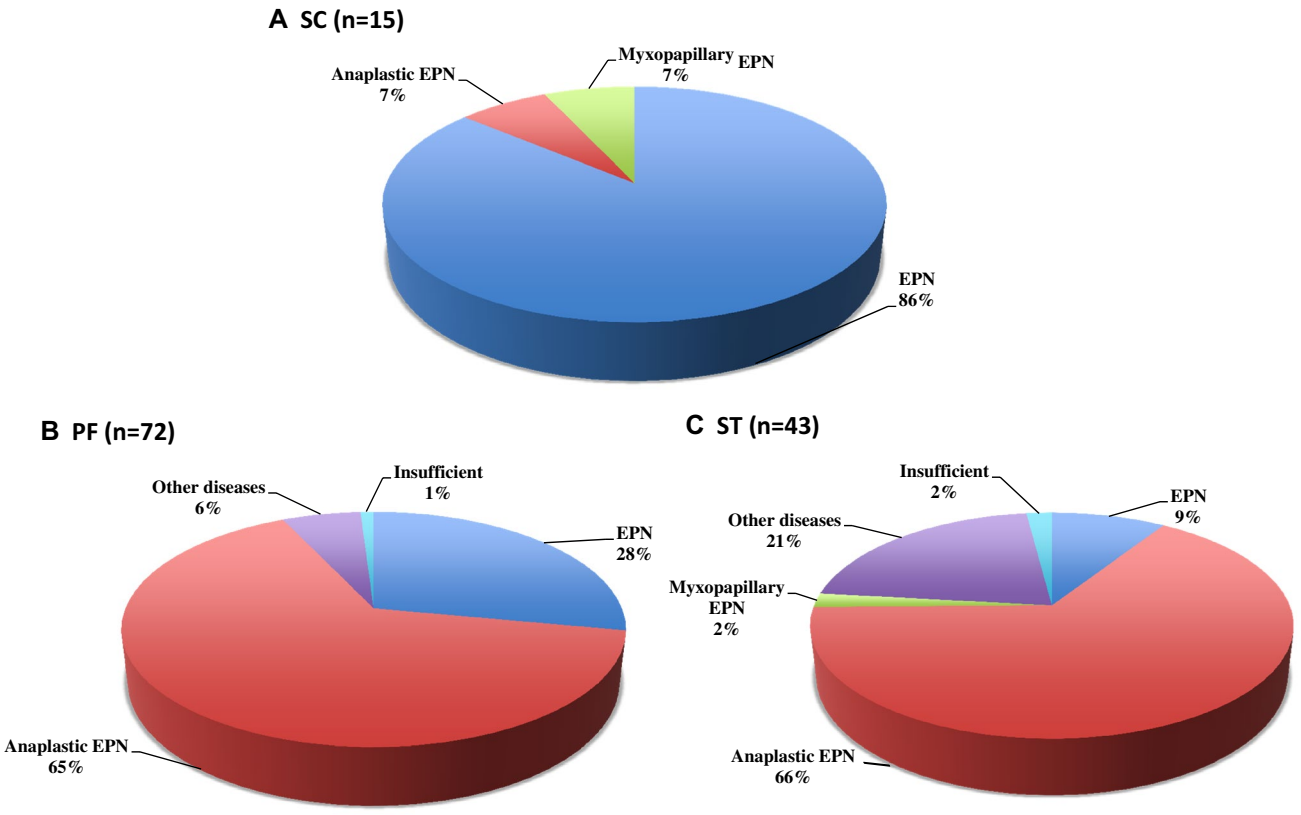

Fig. 1 Proportion of central diagnosis in spinal cord (SC), posterior fossa (PF), and supratentorial (ST) tumors

Table 1 Proposed diagnostic criteria

Ependymoma was defined as a well-demarcated glioma with uniform small cells, round nuclei, a fibrillary matrix, and perivascular pseudorosettes
A diagnosis of anaplastic ependymoma was made when an ependymal tumor shows a markedly increased mitotic activity (10 or more mitoses per 10 high-power fields) or the following three features: (1) a high cellularity, (2) an increased proliferation (5–9 mitoses per 10 high-power fields and/or high MIB-1 labeling index > 10%), and (3) microvascular proliferation or necrosis. High cellularity included focal hypercellular nodules as well as diffuse hypercellularity

(1/29 = 3.0%), and non-RELA/non-YAP1 (9/29 = 31%). Among the cases with consensus diagnosis of ST RELA-negative/YAP1-negative EPNs, four cases demonstrated usual histological features of classic EPN or AEPN, while the remaining cases exhibited evidence of ependymal differentiation as well as variable unusual features, which included astrocytic cells, tanycytic cells, vacuolated cells, or microcysts. Histology and IHC of the representative cases in PF-Grade II-EPN-B, PF-Grade III-EPN-A, and ST-Grade III-*RELA*-positive are shown in Fig. 2.

EPN-RELA

Among the 19 tumors with molecular diagnoses of EPN-RELA, 14 tumors (73.7%) demonstrated a clear cell morphology of the tumor cells, which was accompanied by a rich network of branching capillaries (Fig. 3a), and all cases were recorded as AEPN WHO Grade III. In EPN-RELA, the median age at surgery was 13 years (range 1–63), and a significant proportion (44%) of these tumors was found in adults. The location of these tumors was as follows: frontal in 9 cases, parietal in 4, occipital in 3, and temporal in 2; in addition, the tumors in seven cases presented with a cystic component.

Surrogate markers

No reliable staining was found in either LAMA2 or NELL2. All EPN-RELA cases examined by IHC showed membranous staining of the L1CAM antibody, and the diffuse

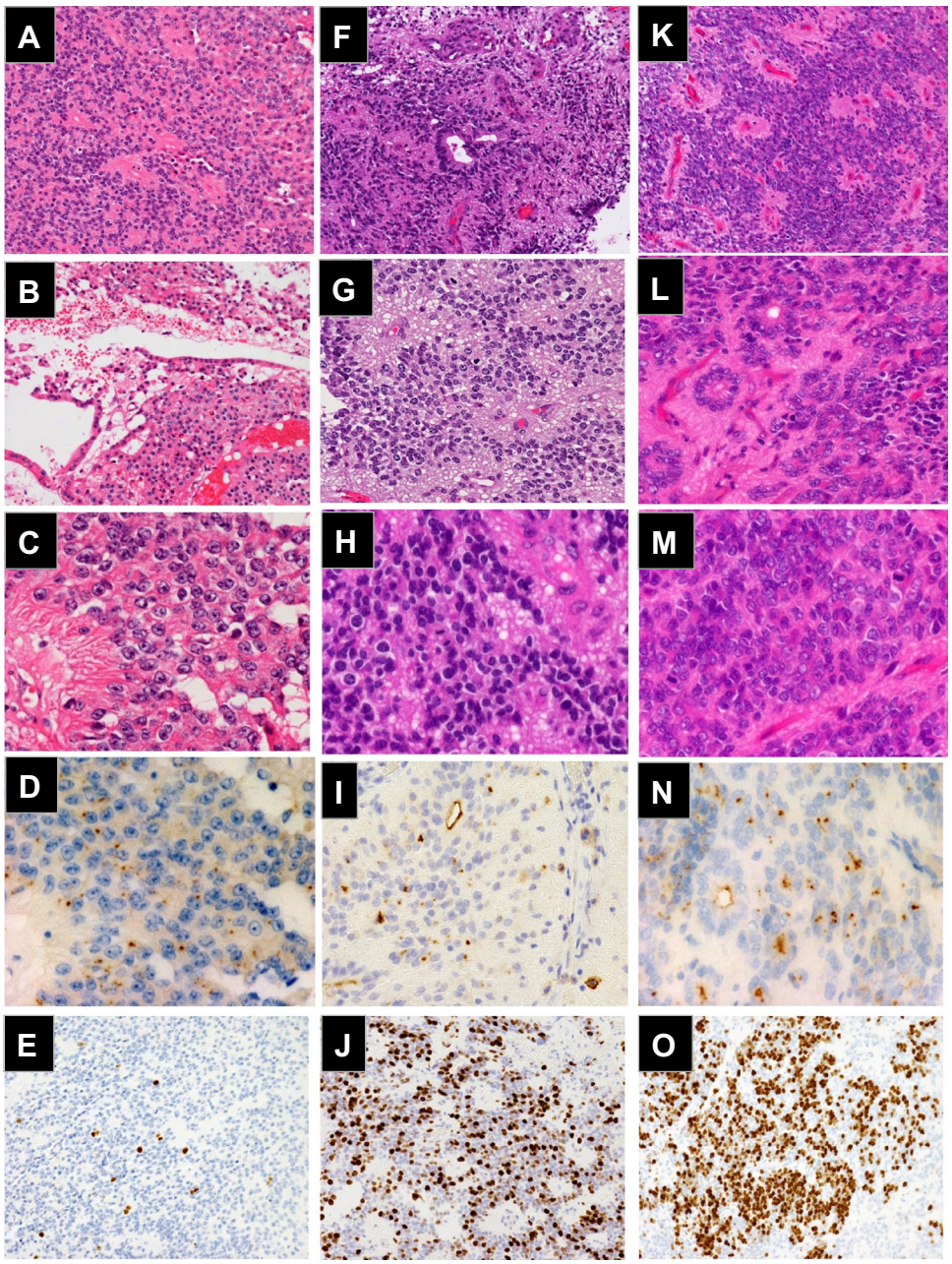

Fig. 2 Histology and IHC analysis of representative cases of PF-Grade II-EPN-B (**a**–**e**), PF-Grade III-EPN-APFA (**f**–**j**), and ST-Grade III-RELA fusion-positive (**k**–**o**). All tumors consistently showed perivascular pseudorosettes that were often accompanied by true rosettes or canals. Increased mitotic activity was observed in cases with Grade III tumors. Note the characteristic positivity for EMA staining. High positivity for MIB-1 was observed in Grade III tumors, but not in Grade II tumors. H&E (**a–c, f–h, k–m**), EMA (**d, i, n**), and MIB-1 (**e, j, o**) staining are shown

expression of L1CAM in the tumor cells, which was usually moderate-to-strong in intensity, was observed in ST AEPNs, not in PF or SC EPNs. We found L1CAM expression in 100% of all 19 EPN-RELAs in which moderate-to-strong expression of the antigen was localized in the majority of tumor cells. No significant expression of the L1CAM antigen was detectable in most of RELA-negative EPNs examined, but the antigen was found in the tumor cells in two cases (one case of YAP1 EPN and one case of non-ependymal tumor).

The results of 12 EPN cases (5 *RELA* fusion-positive and 7 *RELA* fusion-negative) were as follows: all 5 EPN-RELAs showed membranous staining and nuclear accumulation of L1CAM and NF-kB p65 antibodies, respectively (Fig. 3b–d). Both antigens were present regardless of the tumor cell morphology; the antigens were observed not only in clear cells, but also in nonclear cells. L1CAM expression was mostly diffuse and intense, while the nuclear expression of NF-kB p65 was heterogeneous and varied from weak to strong intensity. L1CAM staining was weak in the degenerated or necrotic area of the tumor. In the seven cases of *RELA*-negative EPNs, all cases showed little or no expression of L1CAM. In contrast, five cases had NF-kB p65-positive nuclei in the focal area (> 10%), but two PF AEPNs showed nuclear NF-kB p65 staining in approximately 50% of tumor cells (Fig. 3e). Thus, we rated IHC as positive when at least

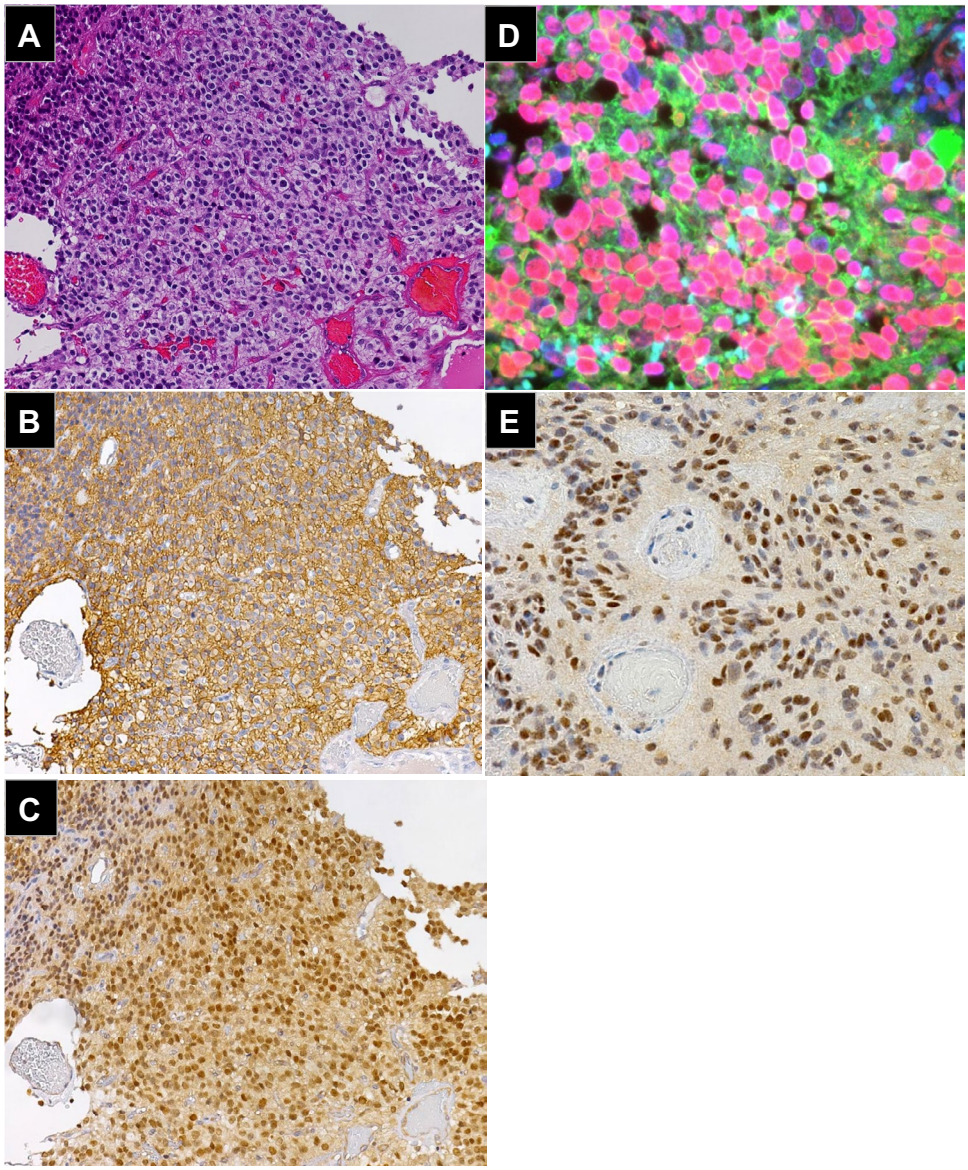

Fig. 3 Expression of L1CAM and NF-kB p65 in *RELA* fusion-positive cases (**a**–**d**) and an *RELA* fusion-negative case (**e**). *RELA* fusion-positive cases exhibited clear cells and a rich network of branching vessels (**a**), diffuse strong membranous expression of L1CAM (**b, d**), and diffuse strong nuclear expression of NF-kB p65 (**c, d**). Nuclear staining with moderate or strong intensity of NF-kB p65 was rarely observed in a PF-Grade III-EPN-A case (**e**). IHC for L1CAM (**b**) and NF-kB p65 (**c, e**). Double immunofluorescence for L1CAM (green) and NF-kB p65 (red) is shown

10% of the tumor cells were equivocally stained. In such scoring, L1CAM had perfect sensitivity (100%, 19/19) and good specificity (95%, 39/41), while NF-kB had perfect sensitivity (100%, 5/5), but was less specific (28.5%, 2/7). In nonneoplastic tissue components, L1CAM expression was occasionally observed in neuropil and neuronal cells, and NF-kB p65 cytoplasmic expression was often present in endothelial cells. The results of the automated Ventana Benchmark platform were similar to those of the manual method.

Prognostic relevance

Patients with PF-Grade III AEPN showed a tendency toward shorter PFS ($p=0.11$), and significantly shorter OS ($p=0.01$) than did those with PF GII EPN (Fig. 4a, b). In 9 patients of PF-Grade II-EPN-A or Grade III-EPN-B patients, one patient (Grade II-EPN-A) died 30 months after biopsy and radiotherapy, and recurrence was found on 3 of 6 PF-Grade II-EPN-A, but not in 3 Grade III-EPN-B patients (Table 2). Both PFS and OS were significantly longer in ST-Grade III EPE-RELAs than in PF-Grade III-EPN-As (data not shown).

Discussion

In this Japanese cohort study, methylation profile grouping was highly consistent with the pathological grading of PF-EPNs given by the consensus pathological diagnoses. The present study indicated that the histopathological diagnosis of PF-EPN by more strict criteria could correlate well

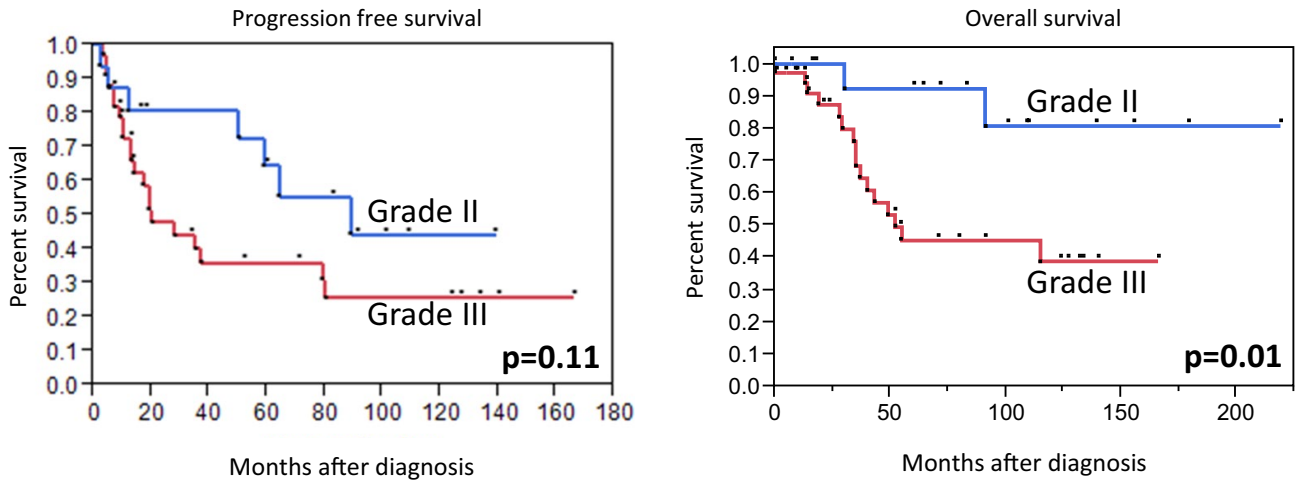

Fig. 4 Histological subgroups of posterior fossa ependymomas display different progression-free survival (PFS) and overall survival (OS)

with the prognosis and molecular classification. Our previous study showed that PF-Grade III-EPN-A tumors were significantly associated with shorter OS ($p = 0.009$) [17]. Our result showing PF-Grade III-EPN-A had the poorest outcome among EPN groups was consistent with that of Pajtler et al. [11]. For PF-EPNs, two distinct molecular subgroups (provisionally termed PF Group A and Group B, or Group 1 and Group 2, or PFA and PFB, or EPN-A and EPN-B) were consistently identified in two independent cohort studies using genetic/epigenetic and clinical features [15, 18]. Patients with Group A (EPN-A) tumors were more frequently classified as WHO Grade III EPNs ($p < 0.0001$, Fisher's exact test) [15], while Group B (EPN-B) tumors were predominantly WHO Grade II [18, 19]. Concordance on the molecular diagnosis and the overall diagnosis of EPNs by expert neuropathologists appeared to be satisfactory.

Distinction between Grade-II EPNs and Grade III-AEPNs is often difficult, with poor interobserver reproducibility even if performed by experienced neuropathologists [7, 20]. In the present study, we established more stringent criteria for defining anaplasia that involved highlighting the use of the Ki-67 labeling index based on the previous studies, and this study underlines the potential interest of assessing the Ki-67 index in adult intracranial EPNs for outcome prediction in the routine diagnostic setting [21–25]. A Ki-67 index < 10% significantly correlated with a better prognosis in PFS and OS rates on univariate analysis in a cohort study of 152 adult intracranial EPNs [6]. Tihan et al. [20] suggested that histological grade (WHO Grade II vs III) is an independent prognostic indicator for event-free survival, but may not be an independent prognostic indicator for OS in pediatric PF-EPNs. Our study showed that PF-Grade III-AEPNs were significantly associated with shorter OS ($p = 0.01$). Thus, histopathological diagnoses by our proposed criteria might be useful in predicting the patient prognosis. However, we found a few patients with Grade II-EPN-A or Grade III-EPN-B patients. In future, further studies with larger number of the discrepant cases are needed.

LAMA2 and NELL2 expression was previously suggested as surrogate markers for PF Groups A and B EPNs, respectively [15]. The present study showed that neither LAMA2 nor NELL2 seems to be a useful, robust marker for routine clinical use. This result was compatible with that of a recent report by Araki et al. [26]. Recently, it was reported that H3K27me3 immunohistochemistry identified Group B with 100% specificity [17, 27, 28]. This method will be useful for the rapid molecular classification of PF-EPN in clinical practice.

Our results indicated that the immunohistochemical pattern of L1CAM and NF-kB p65 could be useful in diagnosing EPN-RELA and that L1CAM might be superior to NF-kB p65 in tumor specificity. EPN-RELA is a genetic EPN subtype defined by the CNS 2016 WHO and accounts for approximately 70% of all childhood ST tumors [10]. L1CAM expression correlates well with the presence of RELA fusion in ST EPNs [10], but the specificity of L1CAM expression, a potential surrogate immunohistochemical marker for this variant, has yet to be fully elucidated [10]. L1CAM expression has been documented in glioblastomas, anaplastic astrocytomas, and gliomatosis cerebri [29, 30]. However, L1CAM expression seems to be nonspecific, as its expression was found in the cell body of the gemistocytes, and no membranous expression was found in the glioma cells. Indeed, our preliminary study showed no expression of L1CAM in astrocytic or oligodendroglial tumors, including glioblastomas (data not shown). We found L1CAM expression in 100% of all EPN-RELAs in which moderate-to-strong expression of the antigen was localized in tumor cells,

Table 2 Characteristics and follow-up in the patients diagnosed as EPN grade II/PFA and grade III/PFB

Patient number	Age at onset	Sex	Consensus pathological diagnosis	Molecular diagnosis	Resection rate of primary tumors including seco look surgery, GTR = 1, STR or biopsy = 0	Radiation field and dose (Gy) at primary treatment, IMRT = intensity-modulated radiation therapy	Recurrence, 0 = negative, 1 = positive	Progression-free period (months)	Prognosis 1: alive 0: death	Observation period (month)
1	6	F	Ependymoma (GII)	PFA	0	Local 50.4	1	5	0	30
2	5	M	Ependymoma (GII)	PFA	0	Local 54	0	16	1	16
3[a]	8	F	Ependymoma (GII)	PFA	No data	No data	1	No data	No data	No data
4	12	F	Ependymoma (GII)	PFA	1	Posterior fossa 50.4	0	7	1	7
5	3	F	Ependymoma (GII)	PFA	1	Local 55.8	0	109	1	109
6	2	M	Ependymoma (GII)	PFA	0	Local 50	1	89	1	156
7	3	F	Anaplastic ependymoma (GIII)	PFB	0	0	0	9	1	9
8	2	M	Anaplastic ependymoma (GIII)	PFB	0	0	0	14	1	14
9	11	F	Anaplastic ependymoma (GIII)	PFB	0	Local 59.4 (IMRT)	0	71	1	71

[a]This patient had a recurrent tumor

although L1CAM was absent in the degenerated or necrotic area of the tumor. L1CAM antigen was rarely detectable in RELA-negative EPNs. On the other hand, the previous studies showed that nuclear immunostaining with anti-NF-kB p65 antibody was reproducibly observed in *RELA* fusion-positive EPN cases [1, 31]. However, Wang et al. showed that the overexpression of NF-kB p65 in 81% of glioblastomas and 65% of anaplastic astrocytomas, and strong nuclear expression of NF-kB p65 in many glioma cells [32]. The authors defined the positive category as tumors exhibiting a strong positive reaction in at least 5% of the tumor cells in one tissue core. In our series, NF-kB p65 nuclear expression varied from cell to cell in EPN-RELAs, and showed a positive reaction in more than 10% of the tumor cells in some RELA-negative EPNs. Thus, we concluded that both L1CAM and NF-kB p65 could be useful as a surrogate marker for RELA-EPNs, and it might be insufficient to rely on positive immunohistochemistry of L1CAM or NF-kB p65 alone for defining RELA-EPNs.

CCE is made up of cells with an oligodendroglial appearance with clear perinuclear halos, and regularly dispersed capillaries that were also geometrically branched and thin-walled were commonly observed [33]. CCEs have been observed in young patients in the ST compartment and may exhibit more aggressive behavior [34]. Not all Grade III CCEs are particularly "clear cell", and in such cases, the designation is based on the cell morphology, pleomorphic nuclei, and number of mitoses [35]. ST RELA-EPN is histologically characterized by a branching network of capillaries and cytoplasmic clearing [10]. A recent study reported that ST clear cell EPNs with branching capillaries were mostly RELA fusion-positive and grade III, and the 5-year PFS and 5-year OS rates were 67.5% and 75%, respectively [12]. Future CNS WHO classification should allow for more narrowly defined tumor groups [36]. Therefore, further studies investigating the molecular, genetic, and prognostic characteristics of ST CCE EPN/AEPNs with/without *RELA* fusion are necessary.

In the present study, the concordance rate of diagnosis between local and central diagnoses was lower in ST EPNs than in PF or SC EPNs. ST cortical EPN is a rare type of EPN. Occasionally, AEPNs can closely mimic glioblastomas. The clear interface between tumor and adjacent brain tissue and the relative uniformity of tumor cell nuclei as well as immunoreactivity for EMA and CD99 support the diagnosis of AEPN as opposed to glioblastoma [37]. Our results were consistent with these pathological findings.

In conclusion, the present study indicated that the histopathological diagnosis of EPN by expert neuropathologists could correlate well with molecular classification in EPNs, and the integrated diagnosis could offer the potential for prognostic evaluation in PF-EPNs. High proliferating activity of tumor cells, such as increased mitotic activity (at least

5/10 HPF) and/or high MIB-1 LI (> 10%), was considered among the most reproducible and reliable criteria for AEPN. The results of the present study consistently demonstrated that the diffuse, strong membranous staining of L1CAM and the nuclear staining of NF-kB p65 in the tumor tissues of EPN-RELAs facilitate the use of L1CAM and NF-kB p65 IHC in the histopathological diagnosis. Our study suggests that the accurate pathological diagnosis of EPN could serve as a first step in treatment decision of each patient and future clinical trials.

Acknowledgements We thank the following individuals for their comments regarding pathological diagnosis: Takashi Komori, Makoto Shibuya, Hiroyoshi Suzuki, and Shinya Tanaka. The authors also thank Tomio Honma and Toshinori Nagai for their excellent technical assistance.

Compliance with ethical standards

Conflict of interest The authors have no conflicts of interest to declare.

References

1. Ellison DW, McLendon R, Wiestler OD et al (2016) Ependymoma. In: Louis DN, Ohgaki H. Wiestler OD, Cavenee WK (eds) WHO classification of tumours of the central nervous system. Fourth Edition revised. IARC press, Lyon, pp 106–111
2. Healey EA, Barnes PD, Kupsky WJ et al Scott RM, Sallan SE, Black PM, Tarbell NJ (1991) The prognostic significance of postoperative residual tumor in ependymoma. Neurosurgery 28:666–671
3. Ikezaki K, Matsushima T, Inoue T et al (1993) Correlation of microanatomical localization with postoperative survival in posterior fossa ependymomas. Neurosurgery 32:38–44
4. Pollack IF, Gerszten PC, Martinez AJ et al (1995) Intracranial ependymomas of childhood: long-term outcome and prognostic factors. Neurosurgery 37:655–666
5. van Veelen-Vincent ML, Pierre-Kahn A, Kalifa C et al (2002) Ependymoma in childhood: prognostic factors, extent of surgery, and adjuvant therapy. J Neurosurg 97:827–835
6. Metellus P, Barrie M, Figarella-Branger D et al (2007) Multicentric French study on adult intracranial ependymomas: prognostic factors analysis and therapeutic considerations from a cohort of 152 patients. Brain 130:1338–1349
7. Ellison DW, Kocak M, Figarella-Branger D et al (2011) Histopathological grading of pediatric ependymoma: reproducibility and clinical relevance in European trial cohorts. J Negative Results Biomed 10:7
8. Pajtler K, Mack SC, Ramaswamy V et al (2017) The current consensus on the clinical management of intracranial ependymoma and its distinct molecular variant. Acta Neuropathol 133:5–12
9. Acquaye A, Vera E, Gilbert MR et al (2017) Clinical presentation and outcomes for adult ependymoma patients. Cancer 123:494–501
10. Parker M, Mohankumar KM, Punchihewa C et al (2014) *C11orf95-RELA* fusions drive oncogenic NF-κB signallimng in ependymoma. Nature 506:451–455
11. Pajtler KW, Witt H, Sill M et al (2015) Molecular classification of ependymal tumors across all CNS compartments. Histopathological grades, and age groups. Cancer Cell 27:728–743
12. Figarella-Branger D, Lachapt-Zalcman E, Tobouret E et al (2016) Supratentorial clear cell ependymomas with branching capillaries demonstrate characteristic clinicopathological features and pathological activation of nuclear factor-kappaB signaling. Neuro-Oncol 18:919–927
13. Nakamura T, Fukuoka K, Ikeda J et al (2017) Encouraging option of multi-staged gross total resection for a *C11orf-RelA* fusion-positive supratentorial anaplastic ependymoma. Brain Tumor Pathol 34:160–164
14. Onishi S, Yamasaki F, Nakano Y et al (2018) RELA fusion-positive anaplastic ependymoma: molecular characterization and advanced MR imaging. Brain Tumor Pathol 35:41–45
15. Witt H, Mack SC, Ryzhova M et al (2011) Delineation of two clinically and molecularly distinct subgroups of posterior fossa ependymoma. Cancer Cell 20:143–157
16. Sasaki A, Yokoo H, Tanaka Y et al (2013) Characterization of microglia/macrophages in gliomas developed in S-100β*v-erbB* transgenic rats. Neuropathology 33:505–514
17. Fukuoka K, Kanemura Y, Shofuda T et al (2018) Significance of molecular classification in ependymomas: C11orf95-RELA fusion-negative supratentorial ependymomas are a heterogenous group of tumor. Acta Neuropathol Commun 6(1):134. https://doi.org/10.1186/s40478-018-0630-1
18. Wani K, Armstrong TS, Vera-Bolanos E et al (2012) Collaborative Ependymoma Research Network. A prognostic gene expression signature in infratentorial ependymoma. Acta Neuropathol 123:727–738
19. Hoffman LM, Donson AM, Nakachi I et al (2014) Molecular subgroup-specific immunophenotypic changes are associated with outcome in recurrent posterior fossa ependymoma. Acta Neuropathol 127:731–745
20. Tihan T, Zhou T, Holmes E et al (2008) The prognostic value of histological grading of posterior fossa ependymomas in children: a Children's Oncology Group study and a review of prognostic factors. Mod Pathol 21:165–177
21. Rezai AR, Woo HH, Lee M et al (1996) Disseminated ependymomas of the central nervous system. J Neurosurg 85:618–624
22. Prayson RA (1998) Cyclin D1 and MIB-1 immunohistochemistry in ependymomas: a study of 41 cases. Am J Clin Pathol 110:629–634
23. Figarella-Branger D, Civatte M, Bouvier-Labit C et al (2000) Prognostic factors in intracranial ependymomas in children. J Neurosurg 93:605–613
24. Wolfsberger S, Fischer I, Hoftberger R et al (2004) Ki-67 immunolabeling index is an accurate predictor of outcome in patients with intracranial ependymoma. Am J Surg Pathol 28:914–920
25. Kurt E, Zheng PP, Hop WC et al (2006) Identification of relevant prognostic histopathologic features in 69 intracranial ependymomas, excluding myxopapillary ependymomas and subependymomas. Cancer 106:388–395
26. Araki A, Chocholous M, Gojo J et al (2016) Chromosome 1q gain ad tenascin-C expression are candidate markers to define different risk groups in pediatric posterior fossa ependymoma. Acta Neuropathol Commun 4:88–97
27. Bayliss J, Mukherjee P, Lu C et al (2016) Lowered H3K27me3 and DNA hypomethylation define poorly prognostic pediatric posterior fossa ependymomas. Sci Transl Med 8:366ra161
28. Panwalkar P, Clark J, Ramaswamy V et al (2017) Immunohistochemical analysis of H3K27me3 demonstrates global reduction in group-A childhood posterior fossa ependymoma and is a powerful predictor of outcome. Acta Neuropathol 134:705–714
29. Tsuzuki T, Izumoto S, Ohnishi T et al (1998) Neural cell adhesion molecule L1 in gliomas: correlation with TGF-β. J Clin Pathol 51:13–17
30. Suzuki T, Izumoto S, Fujimoto Y et al (2005) Clinicopathological study of cellular proliferation and invasion in gliomatosis cerebri:

important role of neural cell adhesion molecule L1 in tumour invasion. J Clin Pathol 58:166–171
31. Pietsch T, Wohlers I, Goschzik T et al (2014) Supratentorial epoendymomas of childfood carry *C11orf95-RELA* fusions leading to pathological activation of the NF-κB signalling pathway. Acta Neuropathol 127:609–611
32. Wang H, Wang H, Zhang W et al (2004) Analysis of the activation status of Akt, NFκB, and Stat3 in human diffuse gliomas. Lab Invest 84:941–951
33. Min KW, Scheithauer BW (1997) Clear cell ependymoma: a mimic of oligodendroglioma: clinicopathologic and ultrastructural considerations. Am J Surg Pathol 21:820–826
34. Fouladi M, Helton K, Dalton J et al (2003) Clear cell ependymoma: a clinicopathologic and radiographic analysis of 10 patients. Cancer 98:2232–2244
35. Tihan T, Burger PC (2016) Ependymoma. In: Kleinschmidt-deMasters BK, Rodriguez FJ, Tihan T (eds) Diagnostic pathology neuropathology, 2 edn. Elsevier, Inc, Salt Lake City
36. Louis DN, Perry A, Reifenberger G et al (2016) The 2016 World Health Organization classification of tumors of the central nervous system: a summary. Acta Neuropathol 131:803–820
37. Liu Z, Li J, Liu Z et al (2014) Supratentorial cortical ependymoma: case series and review of the literature. Neuropathology 34:243–252